Universitat Politècnica de Catalunya (UPC)
Universitat Autònoma de Barcelona (UAB)
Universitat de Barcelona (UB)
Institut de Ciències Fotòniques (ICFO)

http://www.photonicsbcn.eu

Master in Photonics

MASTER THESIS WORK

Early detection of biofilms using low-cost polymeric optical Lab-on-a-chip

Bernat Antúnez Vallès

Supervised by Dr. Xavier Muñoz Berbel, (CNM-IMB, CSIC)
Mr. Tobias Nils Ackermann (CNM-IMB, CSIC)
Dr. Crina Cojocaru (UPC)

Presented on date 9th September 2015

Registered at

Escola Tècnica Superior d'Enginyeria de Telecomunicació de Barcelona

Early detection of biofilms using low-cost polymeric optical Lab-on-a-chip

Bernat Antúnez Vallès
Grup de Transductors Químics, Centro Nacional de Electrónica – Institut de Microelectrònica de Barcelona (CNM-IMB, CSIC), Campus UAB, Carrer dels Til·lers, 08193 Cerdanyola, Barcelona, Spain
E-mail: b.antunez.valles@gmail.com

Abstract. In surface colonization, microorganisms tend to form complex biological structures containing cells and adhesion molecules, called biofilms, which provide them with high stability and resistance to biocide compounds. These biofilms are dynamic structures in which bacteria, individually or in layers, are continuously recruited and released with time. This dynamism makes biofilms a source of microorganism, sometimes pathogens, becoming elements of risk for public health. Up to now, most widespread detection methods for biofilm formation are based on conductimetric, capacitive or potentiometric analyses. These methods are simple, easy to implement and sensitive but prone to false positives for their low selectivity, interference of environmental factors (e.g. temperature or medium conductivity) and ageing/corrosion of the transducer. The aim of this master thesis was to develop a low-cost polymeric optical Lab-on-a-chip for sensitive and selective detection of biofilms in early stages of formation. Lab on a chip consisted of two poly(methyl methacrylate) layers containing two SU-8 waveguides confronted one to the other with a microfluidic channel in between. The region between waveguides was etched with suitable patterns to promote bacterial adhesion and biofilm growth, thus enhancing sensor sensitivity to initial stages of biofilm formation. Sensing principle was based on the changes produced in the spectral response of the system (by absorbing components present in the biofilm) and the amount of light reaching the detector when a biofilm was growing between both waveguides. Optical measurements provided the system with high selectivity allowing to differentiate between water-based elements (such as biofilms), which may confine the light, and salt incrustations (the major interference in electrical analysis systems) which should disperse light. This structure represent a step forward in early detection of biofilm formation, very relevant in several areas such as water distribution, food and beverage industries and even medicine.
Keywords: optical lab on a chip, biofilm detection, micro-patterning, polymeric structure

1. Introduction

Biofilms are biological structures containing microorganisms in which cells adhere to each other on a surface embedded within a self-produced matrix. Biofilm formation begins with the attachment of planktonic bacteria (i.e. bacteria freely moving in a liquid medium) to a surface through Van der Waals forces. This first contact is reversible until a population threshold of fixed bacteria is reached. Then, their phenotypic expression is modified by the action of quorum sensing mechanisms, drastically changing their behavior [1]. They begin to secrete biopolymers (lipids, polysaccharides, external DNA…) that form what is known as extracellular polymeric matrix, which makes the adhesion process irreversible [2]. Successive adhesions and cell divisions create a seemingly random porous structure, but that has functional purposes with channels that facilitate the flux of oxygen, nutrients and signaling molecules [3], and that reach a dynamic equilibrium of growth and dispersion when mature enough to colonize new surfaces. This is schematically illustrated in figure 1.

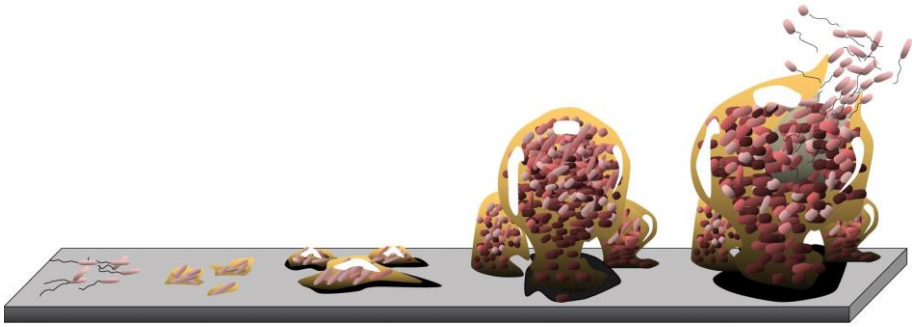

Figure 1. Biofilm formation process: Attachment, irreversible adhesion, maturation and finally dispersion. Image by D. Davis - From: Looking for Chinks in the Armor of Bacterial Biofilms Monroe D PLoS Biology Vol. 5, No. 11

Early adhesions may be initiated for different reasons. Accumulation of nutrients on surfaces is frequent and positively incentives permanent fixation [4]. Hydrophobicity facilitates attachment to rough surfaces, including the extracellular polymeric matrix itself [5]. Once a bacterium is fixed, it receives genes from the already present bacteria through quorum sensing mechanisms that ensure a correct adaptation and contribution to the biofilm, even between species that are not able to grow a biofilm for themselves (for example *Legionella spp.*) [6].

Bacteria inside biofilms have a notoriously increased resistance against detergents and antibiotics [7], making them prevalent in natural, industrial and hospital settings [8][9]. Their presence poses a potential risk to human health in some situations where there is exposure to the liberation of large fragments of biofilm that may carry pathogens [7] [10]. For instance, infections due to biofilms are not rare in hospitals, because patients may have low defenses and the possible presence of antibiotics in low concentrations incentives biofilm formation [11]. This makes their early detection relevant, before any dispersion occurs. Traditionally, the presence of biofilms is not controlled by detection but with the use of biocides. However, they are fully efficient only against planktonic bacteria; if a biofilm is already formed some part of it will remain. Additionally, biocides produce secondary products that may be potentially harmful. For this reason, there has been a lot of work regarding biofilm detection systems [12], more specifically for its implementation in water distribution systems. The majority of systems reported are based on indirect measurements of thermal or mechanical efficiency, or direct methods based on the electric/electrochemical biofilm activity (principally impedance or potentiometric systems) [13]. For instance, a biofilm growing on the internal surface of a capacitor is detected measuring variations in capacitance due to the change in effective dielectric constant. On one hand, indirect systems have low sensibility, only allowing biofilm detection on the late stages of their development (over 40 μm), which makes them inefficient for early detection of sanitary risk in water distribution systems. In addition, they cannot differentiate between biofilms and other adhered compounds, like inorganic salts. On the other hand, systems based on electrical measurements present important stability, durability and reliability problems despite their high sensitivity. They are not very robust since their response is dependent on external factors, such as ambient conditions (temperature changes, ionic charge of the medium, conductivity…), presence of substances with electron transference capability, superficial deposition of compounds, etc. Moreover, the electrode material, generally a metal, can be object of oxidation or surface poisoning by compounds present in the medium, limiting its reliability and durability. Hence, electrochemical sensors are not suitable for long term monitoring in natural environments that may change ambient conditions abruptly. Also important to mention, this devices are expensive which halts an extensive implementation to water distribution systems, thus limiting their application to a small number of key sectors.

Optical measurements have important advantages over previously mentioned methods thanks to their non-invasiveness, lack of ambient dependence, low cost (if based on polymeric materials),

high sensitivity and easy miniaturization. In this work a simple, robust and low cost optical polymeric Lab-on-a-chip is proposed and tested. An optical fiber illuminates a microfluidic chamber, which has a micrometric pattern to facilitate bacterial adhesion, and where a suspension of *Pseudomona putida* in minimum medium AB is introduced to grow a biofilm. Aligned to its bottom part a bent SU-8 waveguide of 40μm thickness gathers light that passes through any existing biofilm (plus some scattered light contribution from the surroundings), and directs it to an optical fiber tilted 90^{o} from the original direction and connected to a spectrometer.

2. Materials and Methods

2.1. Chip design and fabrication

An optical Lab-on-a-chip has been developed for the detection of biofilm formation. The proposed device consists of a two-layer poly(methyl methacrylate) (PMMA) microfluidic chip (figure 2a). The bottom layer contains the optical elements, concretely a SU-8 bent waveguide (4mm bend rad.) of rectangular section (240μm width, 40μm height) and a straight SU-8 rectangular waveguide (50μm width, 40μm height) facing each other at a distance of 300μm. Between both waveguides, chip presents a micrometric pattern to promote bacterial attachment and subsequent biofilm formation. Bent waveguide ensures reduction of the number of interfering non-confined rays reaching the detector, thus improving signal-to-noise ratio (SNR). Optical performance of the chip has been theoretically evaluated by ray tracing using TracePro simulation software (Lambda Research, Littleton, MA, USA) with a 3D model of the chip. Optical properties of each component of the chip (i.e. refractive index) have been included considering the data sheet of each material. According to simulations (Figure 2b), bent waveguides provide signal-to-noise ratios close to 60. The greater width of bent waveguide in the design ensures a significant coupling to the straight waveguide. Top layer contains the microfluidic elements; concretely a laser engraved fluidic channel and the fluidic inlet and outlet. Both layers contain alignment features to be able to perpendicularly position the channel between the waveguides.

Fabrication process combines photolithographic steps and laser ablation for obtaining the final structure. First, SU-8 waveguides are deposited on top of the bottom PMMA layer using conventional photolithography methods. Concretely, a soluble SU-8 layer of 40μm uniform thickness is illuminated with the desired UV light pattern (using a mask) to crosslink and fix material exposed to light, posteriorly removing the remaining soluble part. Then, a pattern is engraved by laser ablation in the zone between waveguides using an Epilog 24 Mini working at 5 kHz pulse frequency, 5% power and 20% speed. Fluidic elements are defined in the top layer by laser ablation using the same machine working at 5 kHz pulse frequency, 20% power and 10% speed. Both layers are bonded by solvent assisted bonding, first introducing them in an acetone vapor bath during one minute. Then, they are aligned and kept under 5,8 kN pressure at 110^{o} C during 8 minutes. Heating is turned off and pressure is gradually reduced to 0,2kN during 25 minutes. Cooling at room temperature continues until 50^{o}C are reached and joint layers can be manipulated. Final structures are then released by laser ablation at 5 kHz pulse frequency, 100% power and 6% speed (melting and welding the edges of the microfluidic chip for a stronger bond) and observed with a microscope to verify the correct alignment of their parts. These parameters are the result of a previous optimization to ensure an optically clean cut.

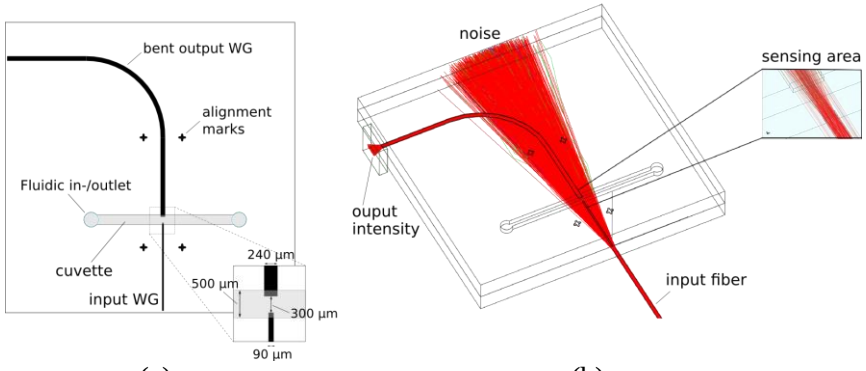

(a) (b)

Figure 2. (a) Sketch of the microfluidic chip including a straight input WG, a bent output WG and a cuvette in between them. Microfluidic pipettes are connected to the fluidic inlet and outlet to introduce samples. (b) Ray tracing simulation considering an optical fiber with NA 0,22 as light source.

2.2. Sensing principle and simulations.

Sensing principle is based on the measurement of coupling loss variations between the two SU-8 waveguides. Having a higher effective refractive index than water, any existing biofilm layer connecting both waveguides without interruptions reduces the angle of aperture for the light beam coming from the straight waveguide, thus increasing the number of photons coupled to the bent waveguide. Bigger layers will further increase coupling until waveguide height (40 µm) is reached, when additional layers reduce vertical confinement caused by the biofilm-water interface, inducing coupling losses. Sensing principle was theoretically validated using TracePro simulation software with the following optical conditions. Biofilm was considered to

be homogeneous, with negligible absorption and with a RI value of 1,39, based on previous publications [14]. Biofilm growth was randomly generated (i.e. random adhesion of cells and local proliferation until producing a mature biofilm). Only in the area between waveguides, due to the presence of the adhesion pattern, bacterial attachment and biofilm proliferation would be considered more probable.

Images of the simulation at different growth stages and their simulated optical losses are shown on figure 3. During the first stages of growth, coupled intensity was decreased until a homogeneous layer covers direct light paths, overcoming scattering effects due to biofilm irregular growth at point (3). Point (4) showed a minor diminution due to the formation of a complete layer over the microchannel which slightly reduced lateral confinement. Subsequent biofilm growth improved coupling until the waveguide height was reached at point (5), from which a biofilm thickness increment caused a reduction in vertical confinement owing to the displacement of the water-biofilm interface (point (6)). Therefore, the described sensing principle could theoretically be used to optically determine the presence of a growing biofilm in the bottom surface of the microfluidic lab-on-a-chip by monitoring changes in coupling losses over time. Enhanced adhesion and growth in the detecting surface enabled an earlier detection. Additionally, it may allow the distinction between biofilms and other adhered structures such as calcareous incrustations which may be highly dispersing and would never present the characteristic loss decrease.

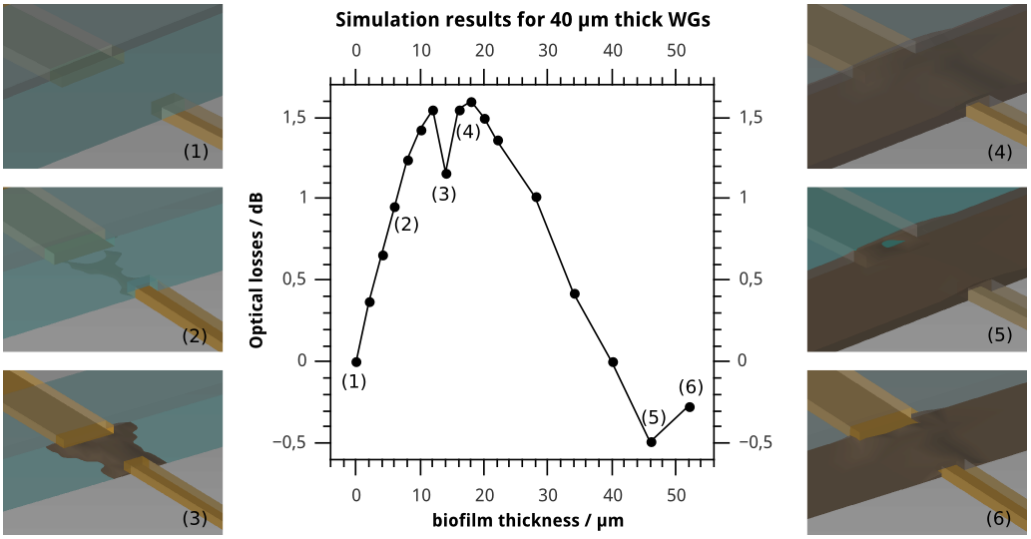

Figure 3. Simulation results are plotted in the central graph, with simulation images included for six representative points: (1) No biofilm, (2) Irregular biofilm, (3) First complete layer in the detecting area induces lateral confinement, (4) Spreading of the layer reduces lateral confinement, (5) Waveguides are completely covered with biofilm, (6) Additional layers reduce confinement.

2.3 Optical measurements

The device presented above was connected to a light source and a spectrometer using a homemade housing. The housing was designed to adapt to the chip, immobilizing it and providing fixation points for the optical fibers, facilitating alignment and manipulation. Two 200µm diameter and 0,22 NA multimode optical fibers were connected to the housing, which was positioned for an optimal coupling to the chip. A halogen light source model HL-2000 and a spectrometer QE65 Pro from Ocean Optics were used as light source and detector for the optical measurements. Recording of data was performed using SpectraSuite software, setting integration time to three seconds, averaging over three measurements to obtain a smoother graph. A box was placed as cover to optically isolate the system, avoiding deviations from the obtained dark reference. Once the setup is stabilized fixing the optical fibers and the device to the table with scotch tape, the microfluidic pipettes were connected to the fluidic inlet and outlet, introducing water with a syringe to obtain a reference spectrum and to detect possible leaks. Water was removed and the sample was introduced, acquiring spectrums every 10 minutes.

2.4 Bacterial culture

To prepare the *Pseudomona putida* suspension, first step was growing an overnight culture in minimum medium AB (MMAB) at 30º C inside a thermic bath agitator. After centrifugation and re-suspension in an adequate volume of minimum medium AB, cell concentration was fixed to 10^8 cell/ml by optical density. Before introducing it into the cuvette, suspension was agitated for a few seconds to ensure homogeneity.

2.5. Fluorescence measurements

Biofilm thickness measurements were carried out using a pseudo-confocal fluorescence microscope. PMMA pieces were introduced in flasks containing bacteria growing with MMAB. At regular times, samples were extracted, carefully washed with distilled water and stained with a live/dead kit (Invitrogen) consisting of a green and a red fluorescent stain. Green stain is membrane permeant and non-fluorescent until activated by intracellular activity whilst red stain only penetrates the damaged membranes of non-viable cells and is activated when fixed to the DNA. Fluorescent emission for activated stains is 30 times greater for red, thus UV illumination is enough to obtain the characteristic green/red images. If desired, longer wavelengths can be used to exclusively excite red stain. Determining the position of top and bottom biofilm layers by focusing them allowed an approximate measurement of biofilm thickness.

4. Results and analysis

Bacterial attachment and biofilm growth depends on many factors. Apart from experimental conditions such as temperature, access to nutrients, oxygenation of the medium, etc., the physic-chemical properties of the support material critically affect the colonization process. In this sense, rough and hydrophobic material should promote bacterial attachment, favoring biofilm formation. Regarding that, biofilm formation on PMMA samples with and without SU-8 waveguides was evaluated in the laboratory under optimal biofilm formation conditions (i.e. with minimal medium, nutrients restriction and without oxygenation). PMMA samples were introduced in flasks containing 10^8 cell/ml of *Pseudomona putida* in MMAB supplemented with glucose (0,2% w/v) and incubated at 30º C for 1 week without further nutrient addition. Samples were regularly extracted measuring biofilm thickness with a pseudo-confocal fluorescence microscope after staining, as previously described. Results are summarized in figure 4.

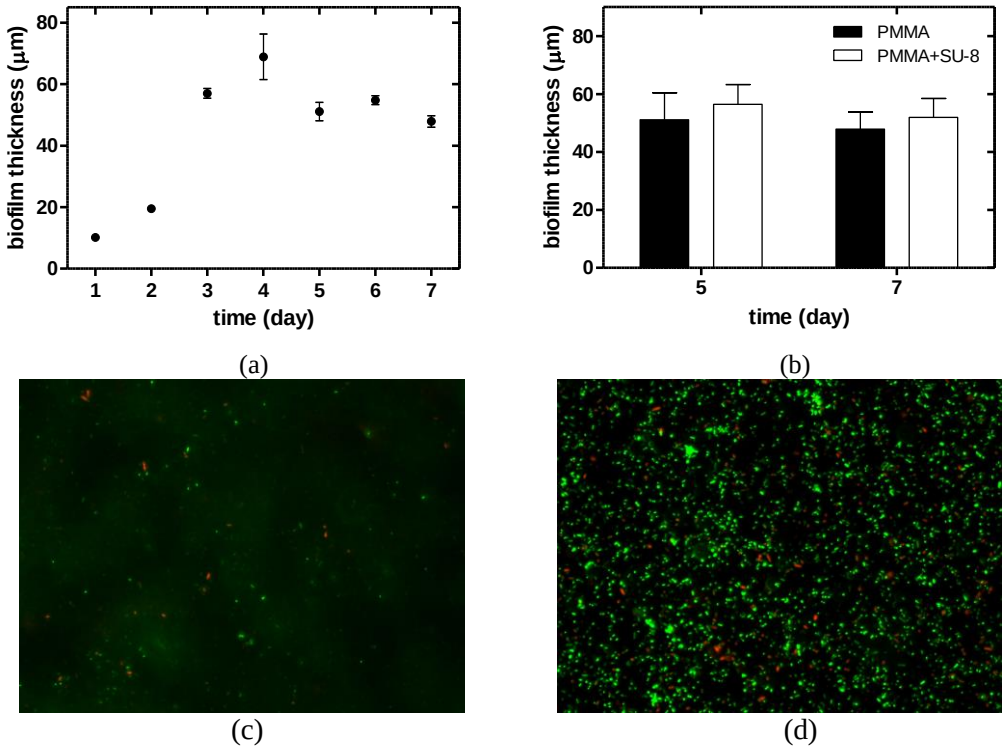

Figure 4. (a) Measured biofilm thickness over time for *Pseudomona putida* on PMMA. (b) Comparison of biofilm thickness in PMMA samples containing SU-8 waveguides and without waveguides. Fluorescent images of PMMA samples after staining with the live/dead kit after (c) one and (d) 4 days of growing. Error bars represent standard deviation (n=3).

As shown in figure 4a, biofilm thickness increased with time until saturation after 3 days, when a mature biofilm of 60 µm was obtained. After that, biofilm thickness oscillated between 50 and 60 µm, due to bacterial recruitment and removal processes. No significant differences were observed when comparing samples with and without SU-8 waveguide (Figure 4b), suggesting that this material do not interfere in the colonization process. Regarding biofilm morphology, although initially quite heterogeneous (Figure 4c), mature biofilms on PMMA presented a quite homogeneous distribution of cells which, according to Figure 4d were mainly alive (green). These results confirm the applicability of PMMA and SU-8 as principal components in our biofilm detector.

Biofilm formation may be promoted by modifying the physic-chemical properties of the PMMA surface. Among other possible modifications, an increase of surface roughness should promote initial attachment stages and subsequent biofilm formation [4]. Taking advantage of the

microfabrication processes, laser ablation was used to etch PMMA surfaces generating four micrometric patterns (figure 5, a to d) engraved using different power and speed parameters. Biofilm formation on the pattern after two days of growth was analyzed by following the staining/imaging protocol previously detailed. As shown in figure 5 (e), all patterns benefited biofilm formation and significant differences were observed between the engraved and the non-engraved areas. From a quantitative point of view (figure 5 f, g), best results were obtained at 5% power and 20% speed, providing with biofilms 25 µm thick (5-6 µm thicker than those obtained out of the pattern) and increasing the number of attached cells from 40 cell/µm^2, in non-engraved regions to 160 cell/µm^2 in the pattern. This optimal pattern was selected for the modification of the detection area (i.e. region between both SU-8 waveguides, see figure 5 h) to promote bacterial attachment and improve chip sensitivity. It should be mentioned that this patterning process could be implemented in the same fabrication process without an appreciable increment in fabrication time or cost.

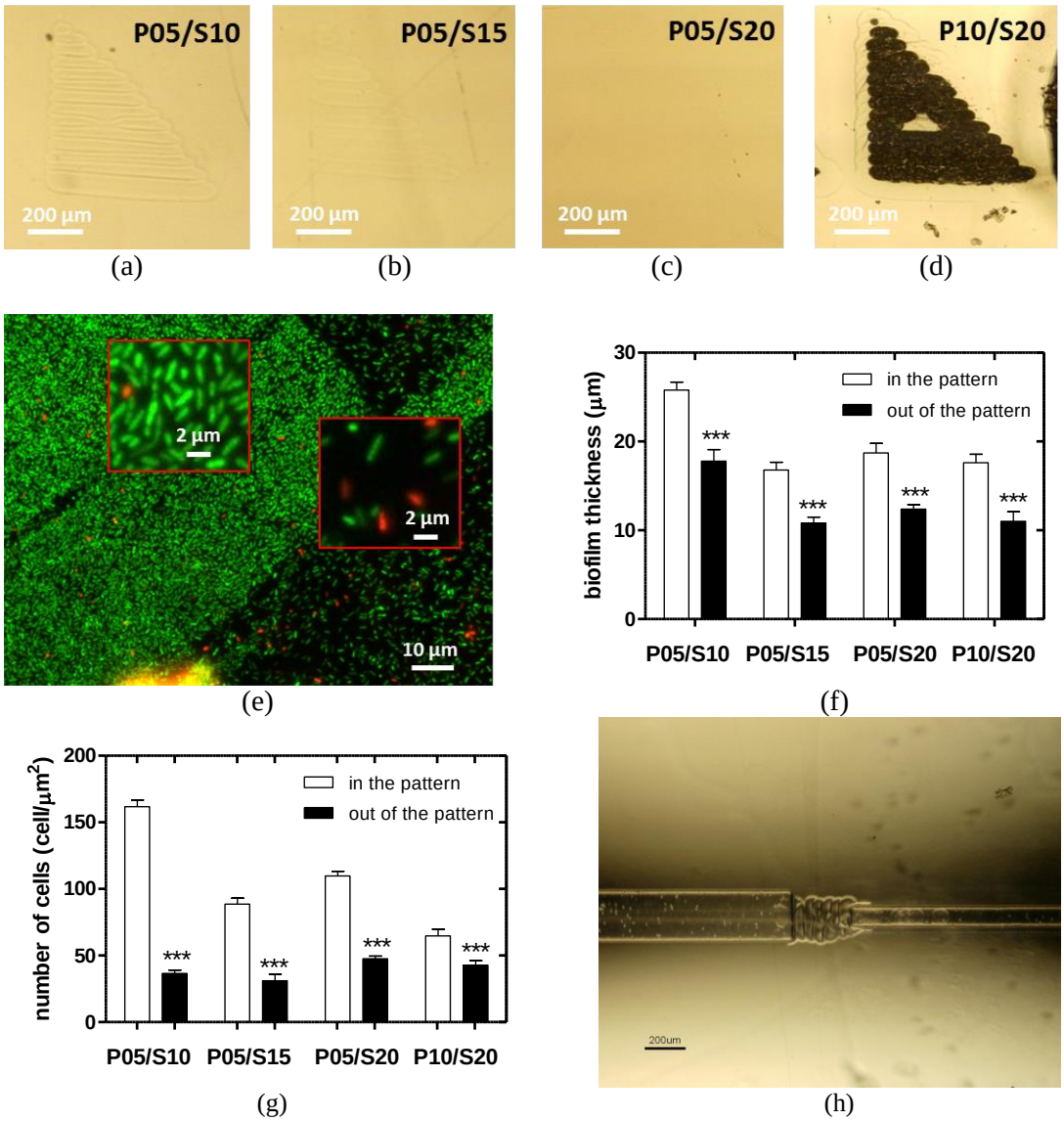

Figure 5. Microscope transmission images of patterns engraved under different conditions: (a) 5% power, 10% speed; (b) 5% power, 15% speed; (c) 5% power, 20% speed; (d) 10% power, 20% speed. (e) Fluorescent live/dead microscope image of patterned and not patterned zones after 2 days of growth on PMMA, for 5% power and 20% speed engraving. (f) Biofilm thickness after 2 days for the different engraving conditions in and out of the pattern. (g) Number of visible cells after 2 days for different engraving conditions in and out of the pattern. (h) Microscope image of the patterned detection zone between SU-8 waveguides. In figures (f) and (g), error bars represent standard deviation (n=3). *** $p<0.001$ compared to values in the pattern.

4.1 Biofilm monitoring

According to simulations, biofilm formation should produce an initial increase in the absorbance magnitude that should be accompanied by a subsequent decrease due to light confinement and guidance though the biofilm structure. Additionally, biofilms formation should also be associated with a change in the spectral response of the system. In this sense, initial planktonic bacteria, most of them individual free-moving cells with a rod-shaped geometry and sizes between 1μm long and 0,5 μm wide on average, should present an absorbance spectrum different than that from a biofilm, where bacteria are aggregated and surrounded by extracellular polymeric matrix. As a first approximation to biofilm growth monitoring, a 10^8 cell/ml suspension of *Pseudomona putida* in MMAB supplemented with 0,2% w/v glucose was introduced in the microfluidic lab-on-a-chip to recreate an accelerated early adhesion process. Absorption spectrums were recorded every 10 minutes for the duration of the experiment (50 hours). Absorbance magnitude (as coupling losses, in dB) is represented with time for 4 representative wavelengths (i.e. 600, 700, 800 and 900 nm) in Figure 6a. Figure 6b illustrates the spectral response of the system (variation of the absorbance with the wavelength) at times ranging from 0 (reference with water) to 50 hours.

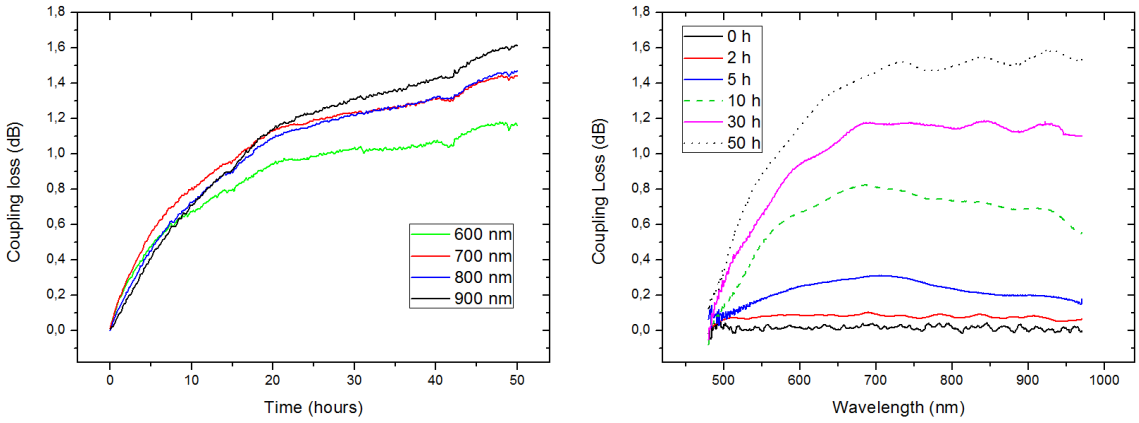

(a) (b)

Figure 6. (a) Representation of the variation of the absorbance with time for 600, 700, 800 and 900 nm.(b) Representative absorbance spectra recorded 0, 2, 5, 10, 30 and 50 hours after cell inoculation in the lab-on-a-chip.

When analyzing absorbance variation with time (Figure 6a), absorbance initially increased until apparent saturation around 50 hours, independently on the analyzed wavelength. This behavior was in accordance with theoretical data from simulations in the initial stages of biofilm formation (Figure 4), where initial attachment and aggregation steps were expected to increase optical losses due to light scattering. Only when a complete a continuous biofilm layer was formed between both waveguides, the tendency was reverted increasing the amount of light collected and decreasing optical losses. This process, theoretically hypothesized by simulation, was not observed experimentally. The reasons for that are still under considerations, although some plausible explanation may be: (i) the short duration of the experiment, which had to be stopped by technical problems after 50 hours, may not be enough to reach the formation of a continuous biofilm layer between waveguides; or (ii) the simulation conditions, full of approaches and simplifications, may be too optimistic and difficult to obtain experimentally. Additional experiments would be necessary for clarification.

From 2 to 10 hours absorbance magnitude quickly increased, probably due to cell proliferation and sedimentation at the bottom of the chip. At these times, the spectral response of the biological system presented an absorbance band centered at 700 nm. This band may be attributed to the randomly oriented suspended cells, which with a size between 500 and 1000 nm may produce a wavelength-dependent scattering generating the previously commented

pattern. From this point, and as previously described, the increase in absorbance magnitude became more wavelength-dependent. Concretely, absorbance increases over time was larger for long wavelengths (above 800 nm) than at short wavelengths (below 800 nm). This fact modified the spectral response of the system, which varied from an initial situation with a clear absorption band at 700 nm to another where all wavelengths presented similar absorption and clear bands could not be identified. A plausible explanation to this fact may be the aggregation of cell in the first stages of biofilm formation. Considering that, aggregated bacteria may produce big particles (between 2 and 20 μm in diameter) that would be larger than the wavelength in the whole range. In this sense, these aggregates should produce scattering that, under the experimental conditions in use, should be wavelength-independent. The scattering pattern should coincide with absorbance spectra recorded in this case. It should be noted that spectra obtained between 30 and 50 hours of incubation seemed to present additional absorbance bands. Precisely two bands centered around 840 and 930 nm may be identified. The origin of these bands is unclear, although they may be due to some secreted compound with absorbance capacity produced by the own microorganism during biofilm formation.
Hence, biofilm formation produced changes in the optical properties of the system (optical losses and changes in the spectral response of the system) that may allow a fast, sensitive and selective monitoring of its formation and evolution, even at early stages (i.e. bacterial attachment and aggregation).

5. Conclusions

This master thesis presents the design, fabrication and characterization of a simple, robust and low-cost polymeric lab-on-a-chip for early detection of biofilm formation based on optical transduction. In terms of design, the chip contained a fluidic inlet/outlet, one microchannel and two waveguides for optical measurement. One of the waveguides corresponding to the optical inlet was bent to minimize the number of non-confined rays reaching the detector and thus the SNR, which was higher than 60. To improve sensitivity, the region between waveguides (i.e. sensing area) was micropatterned to promote bacterial attachment and biofilm formation. From ray tracing simulations, the formation of the biofilm in the sensing area (between both waveguides) should produce an initial increase in the absorbance magnitude, followed by an important decrease when the biofilms was completely covering the area between waveguides. This behavior, theoretically predicted, should allow differentiation between biofilms and saline incrustations, the most common interference in biofilm monitoring. Experimentally, PMMA and SU-8 were chosen as constituent materials. PMMA was selected for presenting ideal properties for biofilm formation such as biocompatibility and hydrophobicity, being capable to induce the formation of biofilms in less than one week. The presence of SU-8 waveguides did not modify the biofilm formation kinetics. Hence, this material may be implemented in the chip structure without altering sensing capabilities. A notable increase in bacterial adhesion and biofilm growth rate was obtained in the micropatterned regions of PMMA, particularly when engraving at 5 % power and 20 % speed. When modifying the region between waveguides of the lab-on-a-chip with a micropattern at these conditions, absorbance increased with time as expected by simulations in the initial stages of biofilm formation. Only the posterior absorbance decrease when the biofilm is mature and optically continuous was not recorded, probably because the monitoring was not long enough. Additionally, spectral response of the system was observed to change from typical small particle scattering spectra, for particles smaller than the wavelength, to a wavelength-independent scattering spectrum. This change was associated to aggregates formation as a first stage of biofilm formation. Future work includes further experiments of longer duration including a continuous flux over the detecting zone to avoid the interference of cell decantation; and implementation of the system in a real but controlled environment, such as water treatment pilot plant.

References:

[1] An D, Parsek MR 2007 The promise and peril of transcriptional profiling in biofilm communities. *Current Opinion in Microbiology* **10** (3): 292–6.

[2] Cynthia B. Whitchurch, Tim Tolker-Nielsen, Paula C. Ragas, John S. Mattick 2002. Extracellular DNA required for biofilm formation. *Science* **295** (5559): 1487

[3] Stoodley, Paul; Dirk de Beer and Zbigniew Lewandowski (August 1994). Liquid Flow in Biofilm Systems. *Appl Environ Microbiol.* **60** (8): 2711–2716.

[4] Karatan E, Watnick P 2009. Signals, regulatory networks, and materials that build and break bacterial biofilms. *Microbiology and Molecular Biology Reviews* **73** (2): 310–47.

[5] Donlan, Rodney M. 2002. *Biofilms: Microbial Life on Surfaces. Emerging Infectious Diseases.* Vol. 8, No. 9: pg. 881-890.

[6] Molin S, Tolker-Nielsen T 2003. Gene transfer occurs with enhanced efficiency in biofilms and induces enhanced stabilisation of the biofilm structure. *Current Opinion in Biotechnology* **14** (3): 255–61.

[7] Gilbert et al. 2002 Mechanisms of anitibiotic resistance in bacterial biofilms. *Int. J. Med. Microbiol*. **292** 107-113.

[8] Hall-Stoodley L, Costerton JW, Stoodley P 2004. Bacterial biofilms: from the natural environment to infectious diseases. *Nature Reviews Microbiology* **2** (2): 95–108.

[9] Lear, G; Lewis, GD (editor) 2012. *Microbial Biofilms: Current Research and Applications*. Caister Academic Press.

[10] Murga R, Forster TS, Brown E, Pruckler JM, Fields BS, Donlan RM 2001 Role of biofilms in the survival of Legionella pneumophila in a model potable-water system. *Microbiology* **147** (Pt 11): 3121–6.

[11] Hoffman LR, D'Argenio DA, MacCoss MJ, Zhang Z, Jones RA, Miller SI 2005. Aminoglycoside antibiotics induce bacterial biofilm formation. *Nature* **436** (7054): 1171–5.

[12] Maiti PK 2006 Detection of biofilm. *Indian J. Med. Microbiol*. **24** (4):303.

[13] http://www.origalys.com/products/biofilm-monitor-legionella-risk-management

[14] Hongbao Xin, Yayi Li, Xiaoshuai Liu, and Baojun Li 2013. *Escherichia coli*-Based Biophotonic Waveguides. *Nano Lett.* **13** 3408-3413.